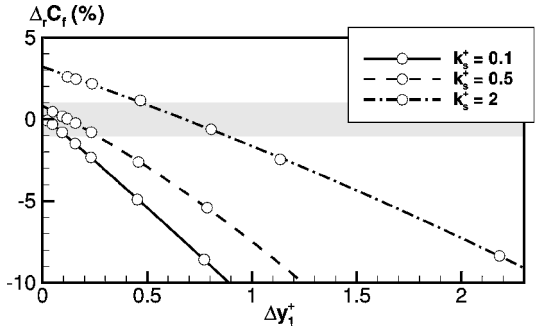

Fig. 4 Deviation of the rough-wall skin-friction coefficient from the smooth-wall value in function of the scaled height of the first cell of the grid (Mach 4, $R_\theta = 8 \times 10^3$).

the limit is the same for two different codes, both based on second-order-accurate numerical schemes. The behavior below this limit is different, with the common point that none of them is desirable.

The preceding section shows that the grid-converged skin-friction coefficient behaves linearly with k_s^+ in the range $k_s^+ = 0 - 10$. This section shows that for a given k_s^+ the height of the first cell off the wall must be at most $k_s^+/2$ in order to avoid a spurious solution. The last question to address is how small the first cell height must be in order to be close to the grid-converged rough-wall solution.

Grid Convergence of the Rough-Wall Boundary-Layer Solution

Figure 4 shows the behavior of deviation (2) for three values of k_s^+ when the grid is refined near the wall. The symbols are the actual results of computations with GASP in the Mach 4 case for $R_\theta = 8 \times 10^3$. The lines are second-order polynomial fits of the computed data. The gray zone represents the range $\pm 1\%$ around the smooth-wall grid-converged value C_{f0}. It is obvious that the smaller k_s^+, the larger the grid-sensitivity of the solution. The values of $C_f(k_s^+)$ reach the limit -1% to C_{f0}, when $\Delta y_1^+ \simeq k_s^+/2$. For k_s^+ below 0.5, the computed solution then stays in the $\pm 1\%$ range when the grid is further refined. However, for k_s^+ above 0.5 (see the case $k_s^+ = 2$ in Fig. 4), the skin-friction value goes on through the $\pm 1\%$ range and reaches the significantly different grid-converged value associated with k_s^+. In each case the 1% limit to the grid-converged rough-wall solution is reached when the first cell height is about 0.2.

In Ref. 4 Menter proposes using the following rough-wall BC for ω: $\beta_0 \omega_w = 60 \nu_w / \Delta y_1^2$. This condition is equivalent to the rough-wall BC equation (1) if $k_s = \sqrt{(N\beta_0/60)}\,\Delta y_1$, which corresponds to a ratio $k_s^+/\Delta y_1^+$ very close to 2 (1.94). As just noted, this relation has the exact effect to keep the solution at the edge $\pm 1\%$ of the smooth-wall value C_{f0} for values of k_s^+ between 0–5 at least: the grid-convergence error compensates for the difference between the rough-wall and the smooth-wall values of the skin-friction coefficient.

Conclusions

The value of the skin-friction coefficient obtained on a flat plate with the $k-\omega$ model and the rough-wall boundary condition for ω is highly sensitive to the scaled roughness height k_s^+. This sensitivity, for k_s^+ below 5, is unphysical. When k_s^+ tends toward zero, the grid-converged computed skin-friction coefficient tends toward the smooth-wall value C_{f0}. The deviation from C_{f0} is directly proportional to k_s^+, with a very weak dependance on the Mach and Reynolds numbers. Namely, $C_f(k_s^+, R_\theta)/C_{f0}(R_\theta) = 1 + (1.8 \pm 0.2)\, k_s^+/100$. This linear relationship is not observed when the grid is too coarse to capture the asymptotic behavior of ω near the wall: with usual second-order numerical methods the first cell height must be smaller than $k_s^+/2$ to avoid spurious or diverged solutions. The observation of the relation $k_s^+/\Delta y_1^+ \simeq 2$ in the range $k_s^+ = 0 - 5$, as recommended by Menter, is sufficient to avoid spurious solutions, but not to get grid convergence. Quite surprisingly, the grid-convergence error in the rough-wall solution yields almost exactly the smooth-wall value of the skin friction. Finally, for the rough-wall skin-friction coefficient to be as close as $x\%$ to the smooth-wall value in a grid-converged way, k_s^+ must be equal to $x/2$, and the first cell height must be below the minimum of 0.2 and $k_s^+/2$.

Acknowledgments

The first author was funded by ONERA and a research fellowship awarded by DGA, the French Armament Procurement Agency, Direction des Systèmes de forces et de la Prospective, under Grant ERE 9960053. The second author was visiting Rutgers University in the framework of an internship from École Polytechnique, supported by the Égide Association from the French Ministry of Foreign Affairs.

References

[1] Wilcox, D. C., "Reassessment of the Scale-Determining Equation for Advanced Turbulence Models," *AIAA Journal*, Vol. 26, No. 11, 1988, pp. 1299–1310.

[2] Menter, F. R., "Influence of Freestream Values on $k-\omega$ Turbulence Model Predictions," *AIAA Journal*, Vol. 30, No. 6, 1992, pp. 1657–1659.

[3] Wilcox, D. C., *Turbulence Modeling for CFD*, 2nd ed., DCW Industries, Inc., La Cañada, CA, 1998, pp. 140–144, 175–177, 343, 344, 461–501.

[4] Menter, F. R., "Two-Equation Eddy-Viscosity Turbulence Models for Engineering Applications," *AIAA Journal*, Vol. 32, No. 8, 1994, pp. 1598–1605.

[5] Nikuradse, J., "Laws of Flows in Rough Pipes," NACA TM 1292, Nov. 1950.

[6] "GASP, General Aerodynamic Simulation Program Version 3," User's Manual, AeroSoft, Inc., Blacksburg, VA, 1996.

[7] Aupoix, B., "Couches Limites Bidimensionnelles Compressibles. Descriptif et Mode d'Emploi du Code CLIC2," ONERA, RF 1/5620.05 DMAE, Toulouse, France, Jan. 1999.

[8] Van Driest, E. R., "Turbulent Boundary Layer in Compressible Fluids," *Journal of Aeronautical Science*, Vol. 18, No. 3, 1951, pp. 145–160.

R. M. C. So
Associate Editor

Turbulent Flow of Power-Law Fluids Through Circular Pipes

Z. U. A. Warsi*
Mississippi State University,
Mississippi State, Mississippi 39762

Nomenclature

a	=	radius of pipe
$F(\tau)$	=	nondimensional $f(t)$
f	=	Fanning friction coefficient for pipes, $\tau_w / \frac{1}{2}\rho \bar{w}_{\text{av}}^2$
$f(t)$	=	pressure gradient, $-\partial \bar{p}/\partial z$
K	=	consistency index
K'	=	$[(3n+1)/4n]^n K$
L	=	section of pipe considered
l	=	l_m/a
l_m	=	turbulent mixing length
n	=	power-law exponent
$\bar{p}$	=	pressure
Q	=	volume flow rate, $\pi a^2 \bar{w}_{\text{av}}$
$R_{e'}$	=	Reynolds number; Eq. (10b)
r	=	radial distance from the centerline
T	=	time used in nondimensionalization
$\bar{T}_{\text{rz}}$	=	Reynolds averaged stress component
t	=	time
u_τ	=	friction velocity, $(\tau_w/\rho)^{1/2}$

Received 31 May 2001; revision received 9 October 2001; accepted for publication 9 October 2001.

*Professor of Aerospace Engineering. Associate Fellow AIAA.

$W = a(n/n+1)(a\Delta\bar{p}/2KL)^{1/n}$
$\bar{w}$ = Reynolds averaged axial velocity
$\bar{w}_{av}$ = velocity averaged over a pipe section
$w^+ = \bar{w}/u_\tau$
y = distance from the wall, $a - r$
$y^+ = \rho y^n u_\tau^{(2-n)}/K$
z = axial coordinate
α, β = parameters in $F(\tau)$
$\Gamma = |\partial\varphi/\partial\eta|^{n-1}$
$\gamma = l^2|\partial\varphi/\partial\eta|$
$\Delta\bar{p}$ = pressure drop
η = nondimensional radial distance, r/a
θ, ψ, λ = functions defined in Eqs. (3) and (5)
ρ = density
τ = nondimensional time, t/T
$\bar{\tau}_{rz}$ = Reynolds stress
τ_w = wall shear stress
φ = nondimensional velocity, $\bar{w}/W$
χ = nondimensional y, y/a
ω, ς = defined in Eqs. (6) and (9)
$(\bar{\ })$ = Reynolds average

Introduction

THE subject of flow of polymeric fluids has of late become of sufficient importance and interest to the science and engineering of aeronautics. It has been known for quite some time that the addition of polymers in Newtonian fluids reduces the drag on bodies in a dramatic way. Much work has been done in the physical and chemical properties of polymers and in the formation of their constitutive equations, e.g., Wilkinson,[1] Bird et al.,[2,3] and Berman,[4] among others. Because most of the polymeric fluids can be approximated, some time quite closely, as power-law fluids, the purpose of this Note is to study the turbulent power-law fluids through circular pipes. A mixing length model for Reynolds stress that is valid in the steady state has been used. Following the leading works of Dodge and Metzner[5] and Wilkinson,[1] a formulation of Prandtl's mixing length for steady-state flow has been proposed in this Note. Numerical solutions of the governing equation of motion have been obtained, both for the startup flow (impulsive start with a constant pressure gradient) and also of a superposed sinusoidal pressure gradient. For the purpose of comparison, the laminar polymeric flow solutions under the same types of pressure gradients have also been reported here. Laminar solutions have been obtained earlier by Edwards et al.,[6] Bird et al.,[7] and Warsi,[8] among others.

Analysis

We start our considerations from the equation of motion of a continuum [e.g., Ref. 9, Eq. (2.33)] and next consider its transformation to orthogonal curvilinear coordinates [Ref. 9, Eqs. (3.115–3.118)]. We take the orthogonal coordinates as the cylindrical coordinates (r, ϕ, z) and introduce the velocity components, pressure, and the stress components as the sum of their mean and perturbation. On taking the Reynolds average of each term and assuming the average of the stress perturbation to be zero, we get the averaged equations. Using these averaged equations for the axial flow through a circular pipe, we obtain the equation

$$\rho\frac{\partial\bar{w}}{\partial t} = f(t) + \frac{1}{r}\frac{\partial}{\partial r}(r\bar{T}_{rz}) + \frac{1}{r}\frac{\partial}{\partial r}(r\bar{\tau}_{rz}) \tag{1}$$

where $\overline{T'_{rz}}$ is neglected. Considering the flow to be that of a power-law fluid, we take

$$\bar{T}_{rz} = K\left|\frac{\partial\bar{w}}{\partial r}\right|^{n-1}\frac{\partial\bar{w}}{\partial r} \tag{2a}$$

where, for a pseudoplastic fluid (solutions of polymers), the exponent $n < 1$. The Reynolds stress is modeled by the Prandtl's mixing length theory as

$$\bar{\tau}_{rz} = \rho l_m^2\left|\frac{\partial\bar{w}}{\partial r}\right|\frac{\partial\bar{w}}{\partial r} \tag{2b}$$

Substitution of Eqs. (2) into Eq. (1) results in the differentiation of absolute values. To circumvent this problem, we change the independent variable r to y, where $y = a - r$. With this change $\partial\bar{w}/\partial y > 0$ throughout from $y = 0$ to $y = a$, we can remove the absolute value sign. Further, introducing the nondimensional variables

$$\chi = y/a, \qquad \varphi = \bar{w}/W, \qquad \tau = t/T, \qquad l = l_m/a$$

and taking

$$T = \frac{\rho a^{n+1}}{KW^{n-1}}, \qquad \frac{Tf(t)}{\rho W} = F(\tau), \qquad \frac{\rho a^n}{KW^{n-2}} = \lambda$$

$$\Gamma = \left(\frac{\partial\varphi}{\partial\chi}\right)^{n-1} = \left|\frac{\partial\varphi}{\partial\chi}\right|^{n-1}, \qquad \gamma = l^2\left(\frac{\partial\varphi}{\partial\chi}\right) = l^2\left|\frac{\partial\varphi}{\partial\chi}\right| \tag{3}$$

while opening the derivatives and changing the variable χ to η through $\chi = 1 - \eta$, we finally have

$$\frac{\partial\varphi}{\partial\tau} = F(\tau) + \frac{\theta}{\eta}\frac{\partial\varphi}{\partial\eta} + n\psi\frac{\partial^2\varphi}{\partial\eta^2} \tag{4}$$

where

$$\theta = \Gamma + \lambda\gamma - 2\lambda\gamma l'/l, \qquad \psi = \Gamma + 2\lambda\gamma/n \tag{5}$$

In this Note we consider the pressure gradient function $f(t)$ in the form

$$f(t) = \Delta\bar{p}/L + \rho c\sin\omega t \tag{6}$$

which covers both the startup flow (case $c = 0$) and the superposed fluctuations over the constant pressure gradient. To obtain $F(\tau)$ defined in Eq. (3), we must assign a form to W. Here we are guided to the form

$$W = n/(n+1)[(1/2K)(\Delta\bar{p}/L)a^{n+1}]^{1/n} \tag{7}$$

which reduces to the value of centerline velocity for the Newtonian case where $n = 1$ and $K = \mu$. With the choice of Eq. (7), the function $F(\tau)$ given in Eq. (3) is

$$F(\tau) = (a^{n+1}/KW^n)f(t)$$
$$= 2[(n+1)/n]^n(1 + \alpha\sin\beta\tau) \tag{8a}$$

where

$$\alpha = \rho cL/\Delta\bar{p}, \qquad \beta = \omega T \tag{8b}$$

Further

$$\lambda = \rho a^n/KW^{n-2} = [(n+1)/n]^{n-2}2^{(n-2)/n}\varsigma \tag{9a}$$

where

$$\varsigma = (\rho a^2/K^{2/n})(a\Delta\bar{p}/L)^{(2-n)/n} \tag{9b}$$

Numerical Solution and Velocity Distribution

A deeper look at the stated problem, which aims at finding the steady-state distribution in polymeric fluids with turbulence, suggests the use of complex approaches with transitional and wall effects with very small grid size near the wall. In this Note, however, we approach the problem by starting the solution from some matching point of the logarithmic layer and consequently use certain results from the pioneering works of Dodge and Metzner, which have been elucidated in Ref. 1. The results from Ref. 1 for the flow of polymeric fluids through a circular pipe are stated in the following and are valid only for the steady turbulent state:

1) Coefficient of friction (Fanning coefficient f):

$$1\Big/\sqrt{f} = (4.0/n^{0.75})\log\left[R_{e'}f^{1-n/2}\right] - 0.4/n^{1.2} \tag{10a}$$

where

$$R_{e'} = \frac{\rho(2a)^n\bar{w}_{av}^{2-n}}{8^{n-1}K'}, \qquad K' = \left(\frac{3n+1}{4n}\right)^n K \tag{10b}$$

2) Near-wall velocity distribution:
In the sublayer $w^+ = (y^+)^{1/n}$, where

$$w^+ = \bar{w}/u_\tau, \qquad y^+ = \rho y^n u_\tau^{2-n}\Big/K, \qquad u_\tau = (\tau_w/\rho)^{\frac{1}{2}}$$

which in terms of $\varphi(\eta)$ is

$$\varphi(\eta) = a(1-\eta)(\rho/K)^{1/n}(u_\tau)^{2/n}\Big/W \tag{11a}$$

where

$$W = \frac{(3n+1)\bar{w}_{\text{av}}}{n+1} \tag{11b}$$

In the turbulent core region the logarithmic velocity distribution in terms of $\varphi(\eta)$ is

$$\varphi(\eta) = \frac{u_\tau}{W}\left[\frac{5.66}{n^{0.75}}\log\left\{\frac{\rho a^n(1-\eta)^n u_\tau^{2-n}}{K}\right\} - \frac{0.4}{n^{1.2}} + \frac{2.458}{n^{0.75}}\left\{1.96 + 1.255n - 1.628n\log\left(3+\frac{1}{n}\right)\right\}\right] \tag{12}$$

All of the formulas (10–12) reduce to the flow of a Newtonian fluid through a circular pipe for which $n = 1$, $K = \mu$.

Having prescribed the values of a, K, L, n, and $\Delta\bar{p}$, first the values of W and $R_{e'}$ through Eqs. (7) and (10) are calculated. The value of $\bar{w}_{\text{av}}$ is available through Eq. (11b). The values of n and $R_{e'}$ are used in the transcendental equation (10a) to compute f. We now choose a value $\eta = \eta_m$ close to 1 where Eq. (12) is applicable. The value of $\varphi(\eta_m)$ from Eq. (12) provides one of the boundary conditions for the solution of Eq. (4). Equation (12) also guides us to choose the proper form of the Prandtl's mixing length. Differentiation of Eq. (12) with respect to η guides us to the Prandtl's mixing length for power-law fluids as

$$l_m = 0.4y/n^{0.25} \qquad \text{or} \qquad l = 0.4(1-\eta)/n^{0.25} \tag{13}$$

It must also be realized that we have posed a time-dependent problem through Eq. (4). For a startup flow the flow is not turbulent in the beginning, but because we are interested only in the steady and periodically nonsteady flows we have arbitrarily introduced a damping factor of time in the value of $\varphi(\eta_m)$ as shown in the numerical example stated next.

For a numerical demonstration we have considered the polymer solution (0.5% hydroxyethylcellulose at 313°K) for which the parameters from Bird et al.[2] are

$$n = 0.595, \qquad K = 0.3\ \text{Pa}\cdot\text{s}^n$$

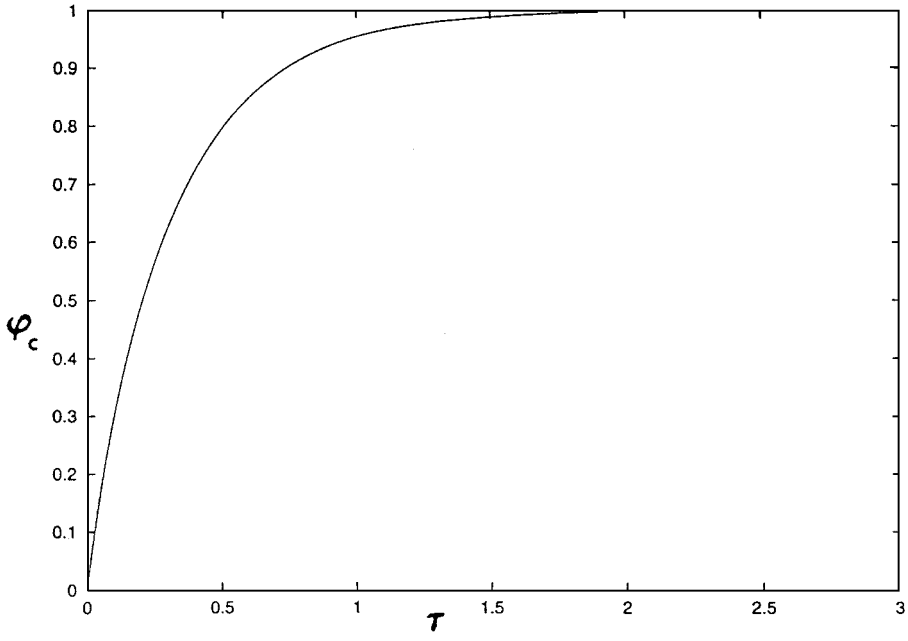

Fig. 1 Centerline velocity of a power-law fluid in laminar flow state with startup condition.

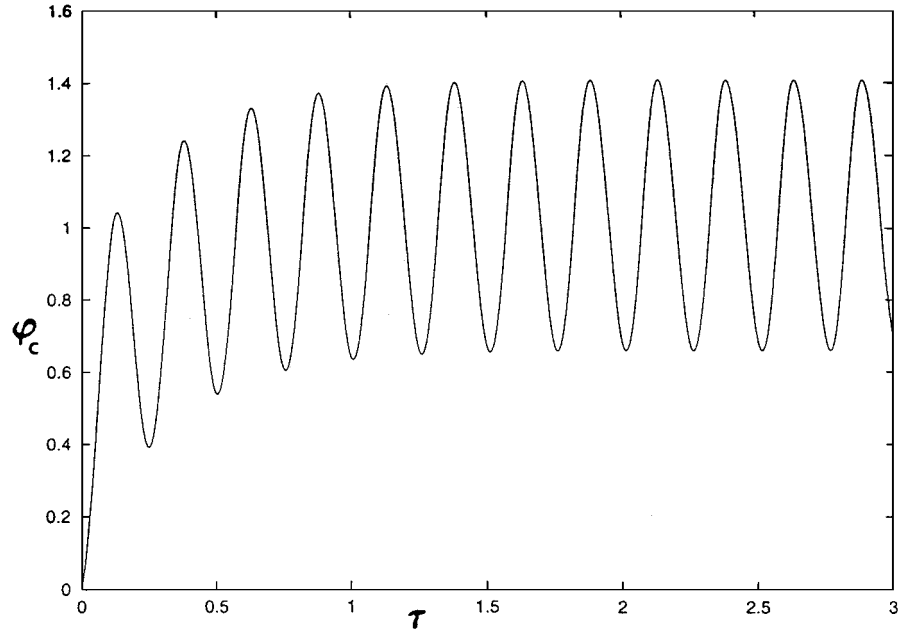

Fig. 2 Centerline velocity of a power-law fluid in laminar flow state with superposed sinusoidal pressure: $\alpha = 2.5$ and $\beta = 25.0$.

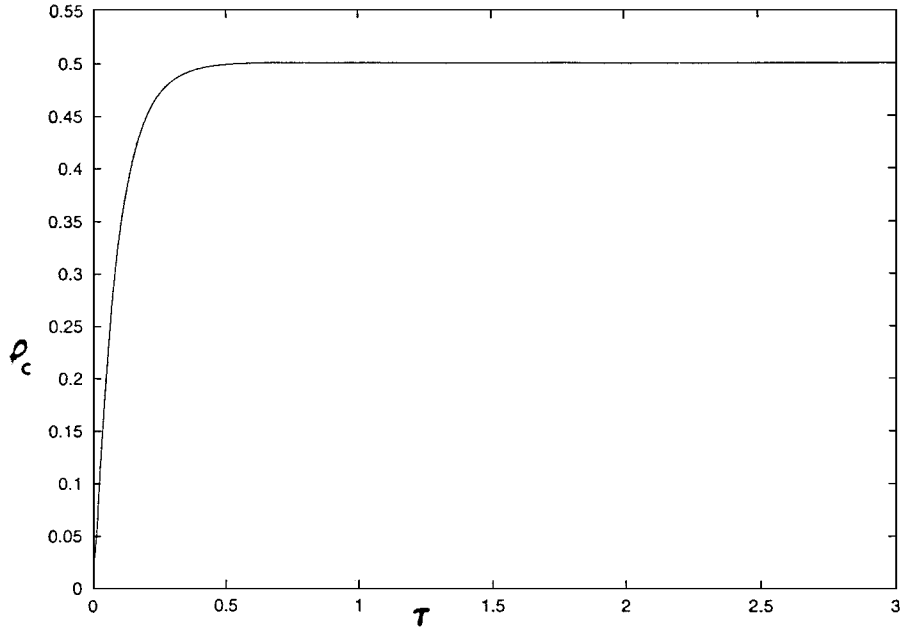

Fig. 3 Centerline velocity of a power-law fluid in turbulent flow state with startup condition.

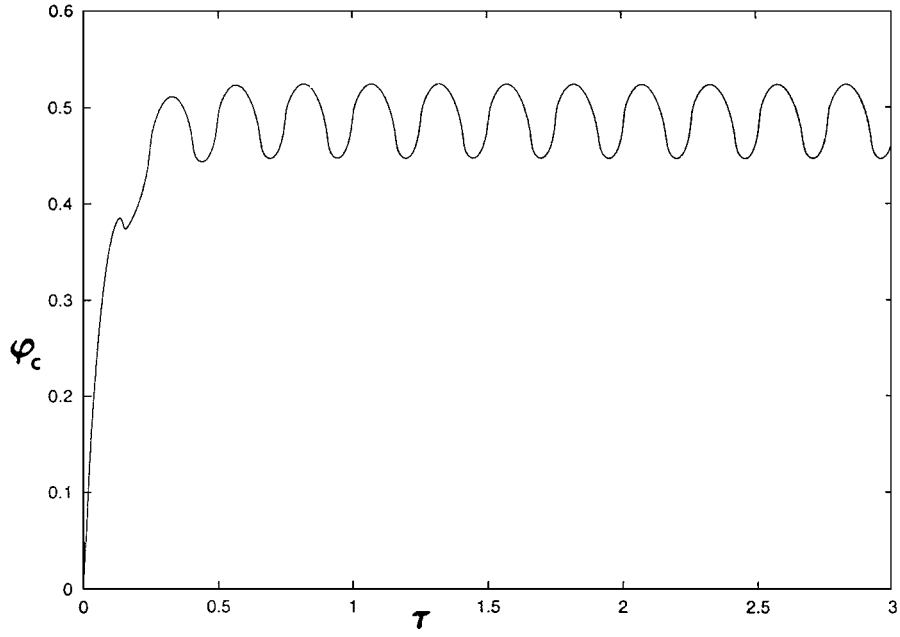

Fig. 4 Centerline velocity of a power-law fluid in turbulent state with superposed sinusoidal pressure: $\alpha = 2.5$ and $\beta = 25.0$.

Further, we have taken

$$\Delta\bar{p} = 1.7\ \text{kPa}, \qquad L = 1\ \text{m}, \qquad a = 3.556\ \text{cm}$$

$$\rho = 1000\ \text{kg/m}^3$$

Calculations using these parameters give

$$f = 0.003122, \qquad W = 30.8703\ \text{m/s}, \qquad R_{e'} = 82{,}729.6$$

(The value of f at the stated value of $R_{e'}$ for Newtonian fluids is $\simeq$0.0046.) The Prandtl's mixing length taken from Schlichting[10] and modified according to Eq. (13) is taken as

$$l = (0.14 - 0.08\eta^2 - 0.06\eta^4)/n^{0.25} \tag{14}$$

In the present calculation we have chosen five grid points, with $\Delta\eta = 0.01$, which are embedded in the sublayer and part of the logarithmic layer. Thus, $\eta_m = 0.95$ at which $\varphi(\eta_m) = 0.476203$. As noted earlier, we make it time dependent as

$$\varphi(\eta_m, \tau) = 0.476203\left[1 - \exp\left(-\tau\sqrt{c_f R_{e'}/2}\right)\right] \tag{15}$$

Thus, the initial and the boundary condition for the startup flow for Eq. (4) are

$$\varphi(\eta, 0) = 0, \qquad \varphi(\eta_m, \tau)$$

prescribed as in Eq. (15). Equation (4) is discretized by using a forward difference in τ and central difference in η The resulting equation is solved by Young's algorithm using Newton's iteration. On the centerline the value of $\varphi(0, \tau)$ is not known, but use has been made of $\varphi'(0, \tau) = 0$. Figures 1 and 2 show the centerline velocity $\varphi(0, \tau) = \varphi_c$ for the startup and superposed fluctuations for the laminar case. Figures 3 and 4 show the centerline velocity $\varphi(0, \tau) = \varphi_c$ for the turbulent case. The preceding data give the reference time $T = 65.302$ s.

Conclusions

Numerical solution of the turbulent flow of polymeric fluids, approximated as power-law fluids, has been obtained for flows through circular pipes. In this Note due advantage has been taken of the empirical formulas for the turbulent flow through circular pipes. A

new mixing length formula for power-law fluids has been proposed. Though the solutions have been obtained from $t = 0$ to the steady state, the transient solution can be considered as a parametric continuation, i.e., nonphysical solution caused by a lack of transition to turbulent flow modeling and transient turbulent modeling. Steady state sets in around $\tau \simeq 0.5$.

References

[1]Wilkinson, W. L., *Non-Newtonian Fluids: Fluid Mechanics, Mixing and Heat Transfer*, Pergamon, Oxford, 1960, pp. 65–70.

[2]Bird, R. B., Armstrong, R. C., and Hassager, O., *Dynamics of Polymeric Liquids, Fluid Mechanics*, 2nd ed., Vol. 1, Wiley, New York, 1987, p. 175.

[3]Bird, R. B., Curtiss, C. F., Armstrong, R. C., and Hassager, O., *Dynamics of Polymeric Liquids, Kinetic Theory*, 2nd ed., Vol. 2, Wiley, New York, 1987, p. 279.

[4]Berman, N. S., "Drag Reduction by Polymers," *Annual Review of Fluid Mechanics*, Vol. 10, 1978, pp. 47–64.

[5]Dodge, D. W., and Metzner, A. B., "Turbulent Flow of Non-Newtonian System," *A.I.Ch.E. Journal*, Vol. 5, No. 2, 1959, pp. 189–204.

[6]Edwards, M. F., Nellist, D. A., and Wilkinson, W. L., "Unsteady, Laminar Flows of Non-Newtonian Fluids in Pipes," *Chemical Engineering Science*, Vol. 27, 1972, pp. 295–306.

[7]Bird, R. B., Stewart, W. E., and Lightfoot, E. N., *Transport Phenomena*, Wiley, New York, 1966, p. 65.

[8]Warsi, Z. U. A., "Unsteady Flow of Power-Law Fluids Through Circular Pipes," *Journal of Non-Newtonian Fluid Mechanics*, Vol. 55, No. 2, 1994, pp. 197–202.

[9]Warsi, Z. U. A., *Fluid Dynamics: Theoretical and Computational Approaches*, 2nd ed., CRC Press, Boca Raton, FL, 1998, pp. 37, 93.

[10]Schlichting, H., *Boundary Layer Theory*, translated by J. Kestin, McGraw–Hill, New York, 1968, p. 568.

R. M. C. So
Associate Editor

Periodic Vibration of Plates with Large Displacements

Pedro Ribeiro*
Universidade do Porto, 4200-465 Porto, Portugal

Nomenclature

$[K_{1b}]$, $[K_{1p}]$	=	linear bending and stretching stiffness matrices
$[K_2]$, $[K_3]$, and $[K_4]$	=	components of nonlinear stiffness matrix
$[M_b]$, $[M_p]$	=	bending and in-plane mass matrices
$[N]$	=	matrix of shape functions
$\{q\}$	=	generalized displacements
u and v	=	in-plane displacements
w	=	transverse displacement
α	=	damping parameter

Introduction

TO characterize the geometrically nonlinear dynamic behavior of plates, it is useful to define their periodic response to harmonic excitations in the frequency range of interest. There are several ways to carry out this task.[1] When finite element (FE) models are used, one often applies the harmonic balance method (HBM)[2] or the incremental HBM.[3] In these methods the number of nonlinear equations to solve simultaneously increases with the number of harmonics used and can be very large. Moreover, the model will be incorrect if the appropriate harmonics are not included in the Fourier series.

The time-domain shooting method[1,4] has two major advantages when compared with the HBM. First, the number of equations to solve is of the order of the original system. Second, it does not depend on an a priori assumption of the number of harmonics present in the motion's Fourier spectrum. Unlike time-domain integration methods applied on their own, like Newmark's method, the shooting technique provides a systematic procedure of calculating the periodic motions in a certain frequency range and converges to stable and unstable solutions. Moreover, the shooting method gives as a byproduct the monodromy matrix, the eigenvalues of which define the solutions' stability.[1]

In this work an algorithm based on the shooting and Newton methods is used to solve the FE equations of motion of isotropic plates. To validate it and to demonstrate that this algorithm has advantages when compared with other methods, results are compared with published ones.

Finite Element Equations of Motion; Shooting and Newton Methods

The hierarchical FE method used to model geometrical nonlinear vibrations of thin, elastic, isotropic plates is described in Ref. 2. The model is derived applying the d'Alembert's principle and the principle of virtual work. Considering stiffness proportional viscous damping,[5] a system of n equations of motion of the following form is derived:

$$\begin{bmatrix} [M_p] & 0 \\ 0 & [M_b] \end{bmatrix} \begin{Bmatrix} \ddot{q}_p \\ \ddot{q}_w \end{Bmatrix} + \alpha \begin{bmatrix} [K_{1p}] & 0 \\ 0 & [K_{1b}] \end{bmatrix} \begin{Bmatrix} \dot{q}_p \\ \dot{q}_w \end{Bmatrix} + \begin{bmatrix} [K_{1p}] & [K_2] \\ [K_3] & [K_{1b}] + [K_4] \end{bmatrix} \begin{Bmatrix} q_p \\ q_w \end{Bmatrix} = \begin{Bmatrix} P_p \\ P_w \end{Bmatrix} \tag{1}$$

or

$$[M]\{\ddot{q}\} + \alpha[K]\{\dot{q}\} + [KNL]\{q\} = \{P\} \tag{2}$$

The subscripts p and b indicate if the vectors and matrices are caused by the in-plane or bending effects.

Only fixed boundary conditions will be investigated, and, because in this case the middle plane in-plane displacements are much smaller than the transverse displacement, the in-plane inertia and damping will be neglected. The excitation vector $\{P\}$ is periodic with excitation frequency ω.

To apply the shooting method, the system of n second-order differential equations of motion (1) is transformed into the following $2n$ system of first-order differential equations:

$$\begin{bmatrix} 0 & [M] \\ [M] & \alpha[K] \end{bmatrix} \begin{Bmatrix} \dot{y} \\ \dot{q} \end{Bmatrix} + \begin{bmatrix} -[M] & 0 \\ 0 & [KNL] \end{bmatrix} \begin{Bmatrix} y \\ q \end{Bmatrix} = \begin{Bmatrix} 0 \\ P \end{Bmatrix} \tag{3}$$

The period can be normalized to unity, by means of transformation $\tau = t/T$, so that the integration time interval is $[0, 1]$. Therefore, the system of differential equations (3) becomes

$$\begin{bmatrix} 0 & [M] \\ [M] & \alpha[K] \end{bmatrix} \begin{Bmatrix} y'(\tau) \\ q'(\tau) \end{Bmatrix} = T \left(\begin{Bmatrix} 0 \\ P \end{Bmatrix} - \begin{bmatrix} -[M] & 0 \\ 0 & [KNL] \end{bmatrix} \begin{Bmatrix} y(\tau) \\ q(\tau) \end{Bmatrix} \right) \tag{4}$$

where the prime denotes differentiation with respect to τ.

By using a $2n$ phase-space vector $\{X(\tau)\} = \{y(\tau), q(\tau)\}$, one can write an initial value problem related to the boundary-value problem (4) as follows:

Received 8 February 2001; presented as Paper 2001-1312 at the AIAA/ASME/ASCE/AHS/ASC 42nd Structures, Structural Dynamics, and Materials Conference, Seattle, WA, 16–19 April 2001; revision received 22 July 2001; accepted for publication 28 August 2001.

*Assistant Professor, Departamento de Engenharia Mecânica e Gestão Industrial, Rua Dr. Roberto Frias. Member AIAA.